Zero-range process with long-range interactions at a *T*-junction

2007 J. Phys. A: Math. Theor. 40 12811

(http://iopscience.iop.org/1751-8121/40/43/001)

IOP PUBLISHING JOURNAL OF PHYSICS A: MATHEMATICAL AND THEORETICAL

J. Phys. A: Math. Theor. **40** (2007) 12811–12828 doi:10.1088/1751-8113/40/43/001

Zero-range process with long-range interactions at a *T*-junction

A G Angel, B Schmittmann and R K P Zia

Department of Physics, Center for Stochastic Processes in Science and Engineering, Virginia Tech, Blacksburg, VA 24061-0435, USA

E-mail: aangel@phys.vt.edu

Received 5 June 2007, in final form 10 September 2007
Published 9 October 2007
Online at stacks.iop.org/JPhysA/40/12811

Abstract

A generalized zero-range process with a limited number of long-range interactions is studied as an example of a transport process in which particles at a *T*-junction make a choice of which branch to take based on traffic levels on each branch. The system is analysed with a self-consistent mean-field approximation which allows phase diagrams to be constructed. Agreement between the analysis and simulations is found to be very good.

PACS numbers: 89.75.−k, 05.70.Ln, 05.40.−a, 05.60.−k

(Some figures in this article are in colour only in the electronic version)

1. Introduction

The zero-range process (ZRP) [1] is a simple model, in which particles hop from site to site on a lattice, that has a soluble nonequilibrium steady state for a number of cases. As such it has been employed extensively as a model for the analysis of nonequilibrium phenomena. Studies have ranged from fundamental investigations of nonequilibrium steady states and phase transitions [2–6] to simple models of real systems such as gel electrophoresis, sandpile dynamics, traffic and compartmentalized granular gases [7–10]. Some interesting properties of the ZRP are the following. It has a soluble nonequilibrium steady state, as stated before, and the statistical weight of configurations in the steady state is described by a product measure. The relative simplicity of this product measure form makes the steady state highly amenable to analysis. The ZRP also displays condensation transitions where a finite fraction of the particles in the system condenses onto a single site. Of particular interest is the fact that these transitions can take place on a one-dimensional lattice, something that would not be expected for an equilibrium system without long-range interactions. In homogeneous systems these phase transitions can be of a spontaneous symmetry breaking nature, something that has been exploited in traffic models as a possible mechanism for the 'jam from nowhere' phenomenon

[11, 12]. The ZRP has also been proposed as a generic model for domain dynamics of one-dimensional driven diffusive systems with conserved density, through which it provides a criterion for the existence of phase separation in such models [13].

Recently, several generalizations of the basic ZRP have attracted much attention in the literature, from both fundamental and application standpoints. One such generalization is a system with open boundary conditions, which can display condensation in cases where none exists for the periodic ZRP [14]. Systems with multiple species of particles have been proposed to study inter-species mechanisms which can lead to new condensation types [15–18] and to model weighted directed networks [19]. The ZRP has also been generalized to continuous masses, and a general criterion for phase transitions could be stated [20–23]. One aspect that has long been known is the fact that the ZRP can be solved on an arbitrary lattice [1], i.e., with a prescribed set of probabilities for a particle to hop from one particular site to another. This has been generalized recently to continuous masses [24]. ZRPs on complex networks have also attracted much attention recently [25–29]. For an overview of the ZRP and many of its generalizations see [2].

The aim of this work is to investigate the ZRP with limited long-range interactions. Specifically, we study a ZRP on a ring lattice, a section of which consists of two branches, with T-junctions at both ends. The rates for a particle at the junction to take one branch or the other are based on the total numbers of particles on the branches. Another way of looking at this is a ZRP on an evolving lattice, with the evolution of the lattice dependent on the state of the system. While the connectivity of the sites is fixed, the probability of particles taking a particular branch at the junction changes dynamically with the state of the system. Thus, the structure of the lattice is static, but the properties of some of the links are allowed to change. Many real systems involve processes which take place on evolving lattices or networks. Food webs constitute one example—see, e.g., [30]—with the network reflecting predator-prey or 'who eats whom' relations. Clearly, these interactions will change with time. For example, if one species is near extinction, its predators will preferentially prey on other species, or even begin preying on new species entirely. Another example is a traffic network; here the structure of the network is largely fixed, but the route which a driver is inclined to take may change depending on the levels of traffic in various parts of the system and any traffic calming measures that are employed (e.g., lanes reserved for buses only during peak times).

Often problems posed on evolving networks, possibly with long-range interactions, are difficult to solve. Thus, it will be helpful to identify simple exactly or approximately *soluble* models on such evolving networks or lattices. They can contribute important steps towards the understanding of such systems.

The paper is organized as follows. In section 2, the model studied is introduced; in section 3 the model is analysed using the solution of the ZRP on a fixed arbitrary lattice as the starting point for a mean-field treatment; extensive numerical results are presented in section 4; finally, in section 5, the implications of this work are discussed and conclusions are drawn.

2. The model

The simple model studied in this paper is defined as follows. Particles hop from site to site on a lattice which consists of a 'main stretch' of L_m sites, branching at a T-junction into two other lanes: labelled 'left' and 'right' branches, with L_ℓ and L_r sites, respectively. At the end, these branches converge to rejoin the main stretch (figure 1). Since the system is periodic, the total number of particles on the lattice, $N_{\rm tot}$, is fixed. There is no exclusion, so that each

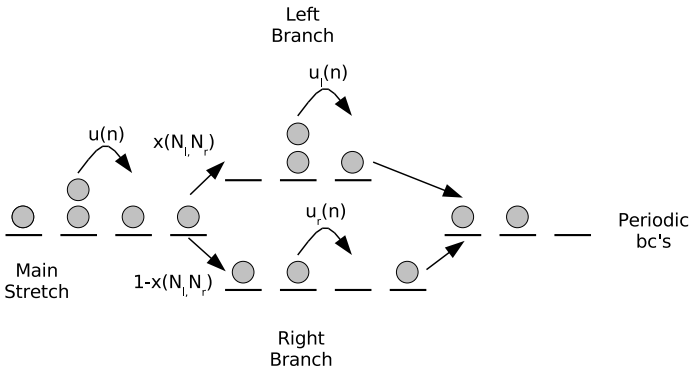

Figure 1. Diagram of the basic system. The lattice consists of a main stretch which splits into two branches (denoted as left and right) at a T-junction before later rejoining. The branches may have different hop rates and different lengths. At the first junction, particles hop to the left or right branches with probabilities that depend on the total numbers of particles in each branch.

site can hold any number of particles. The state of the system is completely described by the set of site occupancies $\{n_i\}$. Particles hop from a site i with a rate $u_i(n_i)$, i.e., a rate dependent on the number of particles at that site, n_i. This corresponds to a particle on site i hopping with a probability $u_i(n_i)\,\mathrm{d}t$ in a suitably small time interval, $\mathrm{d}t$. Particles hop to the rightmost adjacent site, except at the T-junction, where a particle hops to the left branch with a probability x and to the right branch with a probability $1-x$. If x is a constant, then this system can be solved using results for the ZRP on an arbitrary network [1, 3]. In this work, we extend the model to cases where x depends on the number of particles in the left branch N_ℓ and/or the number of particles in the right branch N_r. Thus, x changes dynamically with the configuration of the system.

To keep our model as simple as possible without being completely trivial, we take rates that are uniform within each section and proportional to the standard ZRP form $u(n) = 1 + b/n$, with $b > 2$ so as to produce condensation in the ordinary case [3, 4]. Specifically, we choose, for the main stretch, left branch and right branch, respectively

$$u_m(n) = u(n) \tag{1a}$$

$$u_\ell(n) = pu(n) \tag{1b}$$

$$u_r(n) = qu(n), \tag{1c}$$

where p and q are constants. The most general scenario involves arbitrary (positive) p, q. In this work, we restrict our simulations and analysis to the unit square in the p–q plane. Our main aim is to investigate what happens when a particle at the T-junction has advance knowledge of the states of the branches and stochastically selects which branch to take on the basis of this knowledge. An obvious case to consider is some repulsion from highly occupied branches. In particular, one can consider the case in which a particle only has knowledge of the state of one branch. It turns out that this situation is one of the simplest to treat analytically. An example of such a system is a car faced with the choice between a direct major route with frequent traffic reporting or a longer minor route without any traffic reporting. Heavy traffic may occur on either route and the question is: would it be faster to continue into a known jam or take a longer route with an unknown state? A possible form of x to represent this idea is a

linear dependence on the occupation of the left branch

$$x = \left[1 - \frac{QN_\ell}{N_{\rm tot}}\right]\Theta\left(1 - \frac{QN_\ell}{N_{\rm tot}}\right), \tag{2}$$

where Q is a constant and the Heaviside function, $\Theta(n)$, ensures that x, a probability, does not become negative. Another natural case to consider is the particle making a choice based on the knowledge of the occupations of both branches. A form of x that falls within this category is

$$x = \frac{N_r}{N_\ell + N_r}. \tag{3}$$

This form implies that a particle is more likely to take the branch with the lower occupation, a realistic choice for a driver trying to avoid a jam. Obviously, this choice embodies an extra symmetry, allowing certain simplification in the analysis.

3. Analysis

The simple model defined above is amenable to an approximate analysis based on the solution of the system with a fixed x, the steady state of which is known exactly [1, 3, 31]. As a precursor to the analysis for the variable-x system, results for the fixed-x system are reviewed briefly.

3.1. Fixed-x system

Focusing only on the transitions between 'fluid' (homogeneous) and condensed states, we may exploit the grand-canonical formalism. As in textbook treatments, the number of particles in such an approach is allowed to vary and only the mean number of particles is controlled by the fugacity parameter: z. Within this framework, the steady-state distribution of the occupations of the sites of the system is found to be

$$\mathrm{P}(\{n_i\}) = \frac{1}{Z}\left[\prod_{i\in\mathrm{ms}} f_m(n_i)z^{n_i}\right]\left[\prod_{j\in\mathrm{lb}} f_\ell(n_j)(zx)^{n_j}\right]\left[\prod_{k\in\mathrm{rb}} f_r(n_k)(z(1-x))^{n_k}\right] \tag{4}$$

where the products go over the sites which are in the main stretch (ms), the left branch (lb) and the right branch (rb), respectively. Here,

$$f_\mu(n) = \begin{cases} \displaystyle\prod_{k=1}^{n} u_\mu(k)^{-1} & \text{for} \quad n > 0 \\ 1 & \text{for} \quad n = 0, \end{cases} \tag{5}$$

and obviously, the subscript $\mu = m, \ell, r$ for the ms, lb, and rb, respectively. Finally, Z is a normalization constant, akin to the grand-canonical partition function

$$Z = \sum_{n_1=0}^{\infty}\sum_{n_2=0}^{\infty}\cdots\sum_{n_L=0}^{\infty}\left[\prod_{i\in\mathrm{ms}} f_m(n_i)z^{n_i}\right]\left[\prod_{j\in\mathrm{lb}} f_\ell(n_j)(zx)^{n_j}\right]\left[\prod_{k\in\mathrm{rb}} f_r(n_k)(z(1-x))^{n_k}\right]. \tag{6}$$

With the chosen hopping rates (1), and defining $f(n) \equiv f_m(n)$, we have $f_\ell(n) = p^{-n}f(n)$ and $f_r(n) = q^{-n}f(n)$, so that this expression simplifies considerably

$$Z = \sum_{\{n\}}\left[\prod_{i\in\mathrm{ms}} f(n_i)z^{n_i}\right]\left[\prod_{j\in\mathrm{lb}} f(n_j)(zx/p)^{n_j}\right]\left[\prod_{k\in\mathrm{rb}} f(n_k)(z(1-x)/q)^{n_k}\right]. \tag{7}$$

3.1.1. Condensation transitions in the fixed-x system. Let us first remind the reader that the grand-canonical treatment gives the correct distribution of the system only below a certain critical density ρ_c. Of course, due to the presence of the branches, this quantity will depend on the parameters (x, p, q). To see how this arises, we will need the expression which relates the overall density of the system ($\rho \equiv N_{\rm tot}/L$) to the fugacity z. But we have three sections and the average density of each must be considered separately. To facilitate, let us define

$$g(\zeta) \equiv \frac{\sum_{n=0}^{\infty} n\zeta^n f(n)}{\sum_{n=0}^{\infty} \zeta^n f(n)}, \tag{8}$$

which can be used to relate the density in each section to the effective fugacities

$$z_m \equiv z; \qquad z_\ell \equiv zx/p; \qquad z_r \equiv z(1-x)/q. \tag{9}$$

Summarizing, we write

$$\rho_\mu \equiv \langle N_\mu \rangle / L_\mu = g(z_\mu), \tag{10}$$

so that

$$\rho = \left\langle \frac{N_m + N_\ell + N_r}{L} \right\rangle = \sum_\mu \rho_\mu \frac{L_\mu}{L} \quad = \frac{L_m}{L} g\,(z) + \frac{L_\ell}{L} g\,(zx/p) + \frac{L_r}{L} g\,(z(1-x)/q)\,. \tag{11}$$

At this point, we note that $N_{\rm tot}$ is a fixed parameter of the system and is not equal to the sum of N_ℓ, N_r and N_m as measured in the grand-canonical ensemble at some instant of time.

From our experience with standard ZRPs, it is clear that this approach is valid as long as each effective fugacity remains less than unity (so that Z remains finite). Thus, z cannot exceed the minimum of 1, $p/x, q/(1-x)$. Meanwhile, g is a monotonically increasing function of its argument and, if $g(1)$ is finite, then there will be a density, ρ_c, beyond which (11) has no solution. This happens when the hop rates in each section decay to some constant value β more slowly than $\beta(1+2/n)$ [3, 4]. In the system, the lack of a solution to the density equation manifests itself as a symmetry-breaking condensation transition whereby the excess density will be taken up by a single site. In our case, this site will be located in the section where the effective fugacity first reaches unity. For times much longer than the characteristic time scale associated with individual particles hopping, the condensate will be found on just one site in this section. In simulations starting from random initial conditions, we often observe the condensate to form on the first site of a stretch. However, with other initial conditions, such as a partially nucleated condensate at an interior site or in a segment not expected to hold a condensate, the condensate can form anywhere and we believe that, for finite systems and long times, the condensate will move slowly between sites, eventually exploring all of the possible locations.

To summarize, if $u(n)$ decays more slowly than $1+2/n$, then we can expect condensation for high densities. Further, the condensate will appear in the main stretch if $p > x$ and $q > 1-x$. Otherwise, it will appear on the left or the right branch, depending on whether $p(1-x)$ is less or greater than qx. Though the critical density needed for each of the sections is the same (i.e., $g(1)$), the overall critical density will depend on the details of the parameter set. As an illustration, suppose $x = 0.3$, $p = 0.2$ and $q = 0.8$, so that z should not exceed $2/3$. A condensate will then appear on the left branch when the overall density exceeds $[L_m g(2/3) + L_\ell g(1) + L_r g(7/12)]/L$.

3.2. Varying-x system

The aim is now to use the exact solution of the fixed-x system as a tool to understand the system with the dynamically changing branch choice. The basic assumption is that if the system

relaxes to a steady state, it will do so with some well-defined average value for x. In particular, this assumption is valid if the fluctuations of the particle numbers entering the definition of x, (2) or (3), are not too large. Within this self-consistent mean-field approximation the average numbers of particles in the left and right branches (with the exception of any condensate) can be calculated as a function of x:

$$\langle N_\ell \rangle = L_\ell g(zx/p), \qquad \langle N_r \rangle = L_r g(z(1-x)/q). \tag{12}$$

For our specific hopping rates, g is explicitly

$$g(\zeta) = \frac{\zeta \, {}_2\mathrm{F}_1(2, 2; 2+b; \zeta)}{(1+b) \, {}_2\mathrm{F}_1(1, 1; 1+b; \zeta)}, \tag{13}$$

where ${}_2\mathrm{F}_1$ is the hypergeometric function [32]. Note that $g(1) = 1/(b-2)$, which is finite for $b > 2$ and can provide the quantitative aspects of the phase boundaries. The expressions for $\langle N_\ell \rangle$ and $\langle N_r \rangle$ can then be fed into a self-consistent equation for x. Whether or not this equation admits a solution reveals much about the system. Although the grand-canonical treatment can describe only the sub-critical behaviour of the system in detail, it does lead us to some information about the phase diagram. As we will see, it can predict some simple aspects of the condensed phases. For example, for the fixed-x system, a single condensate appears to soak up all the excess mass in the system. However, for the varying-x system, the feedback mechanism seems to be able to prevent a single condensate from absorbing all of the excess mass. Instead, the excess is shared between two or more condensates.

3.2.1. Branch choice dependent on left branch only. The first case chosen for study has the branch choice probability, x, dependent on the state of the left branch only. For this system, which is defined by the branch choice probability (2), the (self-consistent) equation for the steady-state value of x is

$$x = 1 - \frac{QL_\ell}{N_{\mathrm{tot}}} g(zx/p). \tag{14}$$

This equation depends on both x and z, which are also partially dependent on each other. Within the self-consistent scheme we proposed, both (14) and (11) are to be solved simultaneously in x and z. If a simple solution exists, this implies that there is no condensation. Much like the case for Bose–Einstein condensation presented in textbooks, if the naive approach fails to produce a solution, the specifics of this failure will provide enough information for us to predict where condensation occurs.

Recall that in the fixed-x system the maximum allowed value of the fugacity, z, was $z_{\max} = \min\{1, p/x, q/(1-x)\}$. Thus if (14) can be solved along with (11) under this constraint on z, then there will be no condensation and the number of particles in each section will be known simply by inserting the value of x from the solution into the relevant expression. Note that due to the monotonicity property of g (13) such a solution can be shown to be unique for a given (p, q) pair.

If, under the constraints on z, (14) and (11) cannot be solved simultaneously, but (14) can be solved at $z = z_{\max}$, where $z_{\max}$ is such that the RHS of (11) is as close as possible to N_{tot}, then this implies that a condensate exists but not on the left branch. Recall that in the fixed-x system, inserting z at its maximum value into any of the expressions above provides a correct description of the system except for the condensed site. The location of the condensate can then be determined by inspecting z and $z(1-x)/q$. If $z < z(1-x)/q$, then the condensate appears on the right branch, otherwise it appears on the main stretch.

If neither (14) nor (11) can be solved, even for $z = z_{\max}$, this suggests that x takes a value such that there is a condensation on the left branch. However, this condensation may not be the

same as in the fixed-x system, since the form (2) tends to suppress large numbers of particles on the left branch. In the fixed-x system, the condensate grows indefinitely with increasing total particle density. However, in this varying-x system, an increase in the number of particles on the left branch results in a decreasing value of x. This implies that a condensate on the left branch will not be able to take up the excess density for all densities. In this case, the maximum value of z will be such that either $zx/p = z > z(1-x)/q$ or $zx/p = z(1-x)/q > z$. That is, the system organizes itself into such a state that two coexisting condensates are supported. In the grand-canonical ensemble two sections are critical and both hold a condensate. The locations of the coexisting condensates can be determined from which of z, zx/p and $z(1-x)/q$ are equal, e.g., if $z = zx/p$ then the condensates appear on the left branch and the main stretch.

Unfortunately, the self-consistent and density equations (14) and (11) are often difficult to solve analytically, due to the presence of hypergeometric functions. However, they can be solved numerically and this can be used to map out the phase diagram of the system in the parameters p and q.

The phase diagram becomes particularly easy to calculate if the following two assumptions are made. The number of particles in the system is large enough that the density equation (11) cannot be solved for any allowed values of z and x. Thus there must always be a condensate somewhere in the system. This allows one to assume that z must be at its maximum value of $\min[1, p/x, q/(1-x)]$, instead of numerically solving the density equation. Also, Q is sufficiently large that a condensate cannot appear on the left branch only. The phase diagram of this system can then be mapped out by first assuming a phase, and then working out the values of p and q necessary for its presence.

The phases are identified by the location(s) of the condensate(s) in the system: L for the left branch, R for the right branch and M for the main stretch, while N indicates that no condensates are present in the system. Thus, LR denotes a phase where condensates appear on the left and right branches, for example.

M phase. For a condensate to be present only on the main stretch, z must be equal to 1, both p/x and $q/(1-x)$ must be greater than 1 and the self-consistent equation (14) for x must have a solution. Thus, this phase is bordered by the line $p = \min(x)$, where $\min(x)$ refers to the smallest possible value of x that can be found for (14) in the grand-canonical treatment. It is given by

$$\min(x) = 1 - \frac{QL_\ell}{N_{\text{tot}}(b-2)}. \tag{15}$$

It is also bordered by a line which comes from the solution of the self-consistent equation (14) where $q/(1-x)$ becomes less than 1 indicating a shift to an R phase. This line is given by

$$q = \frac{QL_\ell g(r)}{N_{\text{tot}}}, \tag{16}$$

where $r = (1-q)/p$.

LM phase. For condensates situated on the left branch and the main stretch to coexist, z must be equal to 1, p/x must be equal to 1 (so $x = p$), $q/(1-x)$ must be greater than 1 and the self-consistent equation (14) must have no solution. Thus, this phase is bordered by a line already identified for the M phase ($p = \min(x)$) and also by the line $q = 1 - p$.

LR phase. For condensates situated on the left and right branches to coexist, z must be less than 1, p/x must be equal to $q/(1-x)$, both of these must be equal to z and the self-consistent equation for x (14) must not have a solution. Thus, this phase is bordered by a line already

identified for the LM phase ($q = 1 - p$) and the line $q = (1/\min(x) - 1)p$ which is the border for (14) to have a solution.

R phase. For a condensate to be present on the right branch only, z must be less than 1, p/x must be greater than z and $q/(1 - x)$ must be equal to z. The boundaries for this phase have already been identified as the boundaries of two other phases; this phase is bounded by the line $q = (1/\min(x) - 1)p$ and the line which comes from the solution of the self-consistency equation (14) where x is such that $q/(1 - x) = 1$ which is given by (16).

The other possible phases (L, RM, LRM and N) are not observed when both the density of particles and the repulsion parameter, Q, are sufficiently high, as has been assumed above. For an L phase the density must be sufficiently low, or the repulsion sufficiently weak, to hold a condensate without x becoming too small to sustain it. For an RM phase to be present, there must be some repulsion from the right branch, otherwise the condensate will prefer to form on only one of the sections. For an LRM phase, one must have $z = 1$, $zx/p = 1$ and $z(1 - x)/q = 1$, which can only happen on the line $q = 1 - p$, and even so, it is likely that at least one of the sections will merely be at criticality and not hold a condensate. Finally, for the N phase the density must be so low that there need not be a condensate anywhere in the system.

Assembling all this information together, phase diagrams for given parameters can be produced. As an example, the phase diagram for $Q = 20$, $N_{\rm tot} = 8000$, $L_\ell = 300$, $L_r = 600$ and $L_m = 1000$ calculated via this method is shown in figure 2(*a*). Also shown are some of the values of p and q for which simulations were run to verify the phase behaviour.

It is straightforward to calculate how the phase diagram will be affected by changing the repulsion parameter Q and/or the lengths of the branches. The fact that all the phase boundaries meet at a single point does not change when these parameters are varied; this point is simply displaced. Assuming a sufficiently high density, the line $q = 1 - p$ always forms the boundary between the LM and LR phases; only its length depends on the parameters noted above. The vertical boundary between the LM and M phases is displaced horizontally and its length also changes. For the boundary between the LR and R phases, the slope changes. Finally, the boundary between the R and M phases retains its curved nature, but is displaced and shortened/lengthened.

The theory can also be applied to systems at lower densities and with weaker repulsion, but it is less straightforward. The simplification associated with high density systems—z being pinned to a maximum value—no longer holds. As a result, we must generally rely on numerical methods to find a solution for both equations (14) and (11). With this approach, the phase boundaries can be mapped out, as in the specific case of $Q = 2$, $N_{\rm tot} = 800$, $L_\ell = 300$, $L_r = 600$ and $L_m = 1000$ (figure 2(*b*)). For these parameters, the N and L phases are realized. We also see that the phase diagram has a much richer structure.

A simpler task than computing the full phase diagram for any particle number is calculating how and when the phases emerge. Clearly, at low enough particle number no condensates will be present. The M phase will emerge at $p = q = 1$, when $N_{\rm tot} = L_\ell g(x) + L_r g(1 - x) + L_m g(1)$, with x coming from the solution of $x = 1 - QL_\ell g(x)/(L_\ell g(x) + L_r g(1-x) + L_m g(1))$. For $Q = 2$, this takes place at $N_{\rm tot} = 610$. The L (R) phase first emerges at sufficiently small p (q) when there are enough particles to support such a phase, i.e., $N_{\rm tot} = L_\ell g(1)$ ($L_r g(1)$) and the LR phase when there are enough particles to support both condensates, $N_{\rm tot} = (L_\ell + L_r)g(1)$ and both p and q are sufficiently small. The LM phase will emerge from the $q = 1$ boundary when both the L and M phases can first support condensates at $N_{\rm tot} = L_\ell g(1) + L_r g(1 - x) + L_m g(1)$, where x is given by $x = 1 - (Q/N_{\rm tot})L_\ell g(1)$;

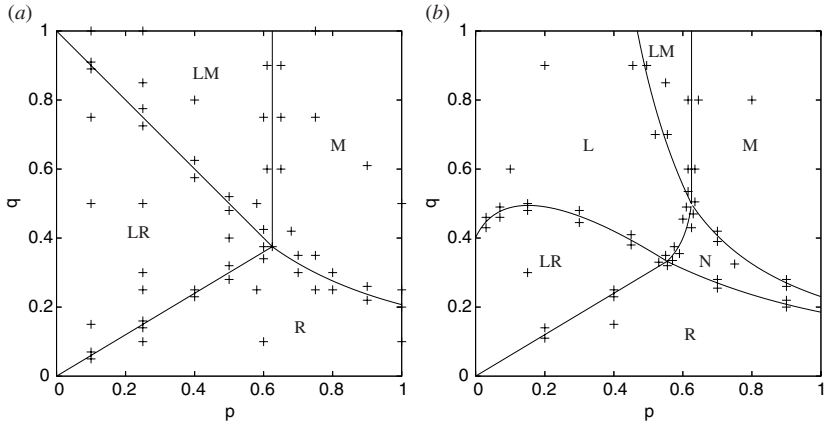

Figure 2. Phase diagrams for the left-branch feedback system with $L_\ell = 300$, $L_r = 600$, $L = 1900$ and (*a*) $Q = 20$, $N_{\text{tot}} = 8000$ and (*b*) $Q = 2$, $N_{\text{tot}} = 800$. Also shown are points where simulations have been run and the expected behaviour verified. The phases are labelled by the position(s) of the condensate(s): L indicates a condensate on the left branch, R indicates a condensate on the right branch, M indicates a condensate on the main stretch and N indicates that no condensates are present.

for $Q = 2$, this is $N_{\text{tot}} = 714$. The R and M phases first meet at the $p = 1$ boundary when $N_{\text{tot}} = L_\ell g(1-q) + (L_r + L_m)g(1)$, with q coming from the solution of $q = QL_\ell g(1-q)/(L_\ell g(1-q)+(L_m+L_r)g(1))$, which in the case $Q = 2$ corresponds to $N_{\text{tot}} = 869$. The N phase disappears when the LR and LM phases meet up at $N_{\text{tot}} = (L_\ell + L_r + L_m)g(1)$, the first point where all three sections can have critical occupancies. The LR and LM phases then begin to border each other along the line $q = 1 - p$, and this line extends as N_{tot} is increased until the L phase is extinguished at $N_{\text{tot}} = Q(L_r + L_m)g(1)/(Q-1)$.

3.2.2. Branch choice dependent on left and right branches. Next, we study the case where the branch choice probability depends on the occupation of both the left and right branches in a repulsive fashion, i.e., the value of x favours sending particles to the least occupied branch. The form used, given in (3), is clearly more symmetric than the previous case. We can write the self-consistent equation for x in a way that makes this symmetry transparent:

$$L_r(1-x)g(z(1-x)/q) = L_\ell x g(zx/p), \tag{17}$$

where we have made the approximation $\langle N_r/(N_r + N_\ell)\rangle = \langle N_r\rangle/(\langle N_r\rangle + \langle N_\ell\rangle)$, which is consistent with the grand-canonical approach used here and should remain valid subject to small fluctuations in the occupations of the branches. Again, the solution of this equation (or lack thereof) in conjunction with the density equation (11) reveals a great deal about the system.

The phase diagram for this system can be mapped out in much the same manner as above, though the analysis is slightly more involved.

As before, simplifications occur if the total number of particles in the system is high enough that a condensate must appear somewhere in the system. Then, the phase diagram can be constructed by assuming the location(s) of the condensate(s) and examining the values of q and p for which a solution can persist. As an example, in order for the system to display a condensate on only the main stretch, we must have $z = 1$ and a solution to the self-consistency equation (17) such that both $x < p$ and $(1-x) < q$.

For a sufficiently large $N_{\rm tot}$, there are three possible ways in which equation (17) cannot be solved for x with a given z. For the system to be in the L, R, or LR phase, we must have $x = p, (1-x) = q$, or $x = p$ and $(1-x) = q$, respectively. By calculating when these equalities hold in conjunction with z being pinned to its maximum value of $\min\{1, p/x, q/(1-x)\}$, the rest of the phase diagram is mapped out.

M phase. As noted above, for a condensate to be present only on the main stretch, z must be equal to 1, both p/x and $q/(1-x)$ must be greater than 1 and the self-consistent equation (17) for x must have a solution. Thus, this phase is bordered by a line which comes from the numerical solution of (17) which in this case takes the form

$$L_r(1-x)g((1-x)/q) = L_\ell x g(x/p). \tag{18}$$

When no solution exists, the system must shift to a phase with a condensate present on one or more of the branches.

L phase. For a condensate to exist only on the left branch, we require $z < 1, z = p/x, z < q/(1-x)$ and no solution to the self-consistent equation (17). Of course, we must ensure that the value of x corresponds to having a condensate in the left branch but not in the right. To find the boundaries of this phase, we consider the conditions for it to shift into a phase with two condensates, one on L and the other on either R or M.

Focusing on the boundary with LR, we arrive at $p/x = z = q/(1-x)$, i.e., $(p+q)\,x = p$ and $z = p+q$. Substituting these into $N_{\rm tot} = \langle N_m\rangle + \langle N_r\rangle + \langle N_\ell\rangle$, we may write $L_m g(z) = L_m g(p+q)$ for the first term, $L_r g(1)$ for the second, but, due to the presence of the condensate, $\langle N_\ell\rangle \neq L_\ell g(1)$. Instead, we assume that (3) remains valid even if one branch contains a condensate, so that $\langle N_\ell\rangle = \langle N_r\rangle\,(1-x)\,/x = \langle N_r\rangle q/p$. Collecting all terms, we arrive at an equation for the L–LR boundary in the p–q plane:

$$N_{\rm tot} = L_m g(p+q) + L_r g(1)(p+q)/p. \tag{19}$$

Similarly, the L–LM boundary is found to be given by

$$N_{\rm tot} = L_m g(1) + L_r g((1-p)/q)/p. \tag{20}$$

R phase. For a condensate to exist only on the right branch, we require $z < 1, z < p/x, z = q/(1-x)$ and the right branch occupation to be greater than critical so that there is no solution to the self-consistent equation for x (17). Following the reasoning above, we find an equation for the R–LR phase boundary:

$$N_{\rm tot} = L_\ell g(1)(p+q)/q + L_m g(p+q), \tag{21}$$

and similarly, one for the R–RM boundary

$$N_{\rm tot} = L_\ell g((1-q)/p)/q + L_m g(1). \tag{22}$$

LM phase. For condensates situated on the left branch and the main stretch to coexist, we must have $z = 1, x = p, 1-x < q$, and no solution to the self-consistent equation for x (17). Thus, this phase is bounded by the line already identified as a boundary for the L phase (20), the line $q = (1-p)$ and a line coming from the numerical solution of (17) which in this case takes the form

$$L_r(1-p)g((1-p)/q) = L_\ell p g(1), \tag{23}$$

and gives the limit of the region in which no solution can be found. This coincides with part of the boundary from the M phase; in fact, the only way in which the equation giving the

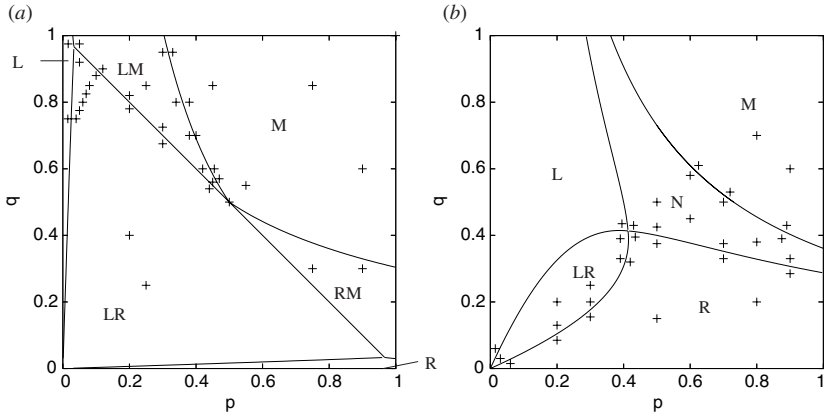

Figure 3. Phase diagrams for the system with repulsive feedback from both branches, with $L_\ell = L_r = 500$, and $L_m = 1000$ and (*a*) $N_{\rm tot} = 8000$, (*b*) $N_{\rm tot} = 800$. Also shown are points where simulations have been run that verify the predicted behaviour. Note that only half of the diagrams have been explored in this way due to the symmetry of the system. The phases are labelled by the position(s) of the condensate(s): L indicates a condensate on the left branch, R indicates a condensate on the right branch, M indicates a condensate in the main stretch and N indicates that no condensates are present.

boundary for the M phase (18) cannot be solved under the high density assumption is if either $x = p$ or $(1 - x) = q$.

RM phase. Similarly, for condensates situated on the right branch and the main stretch to coexist, we must have $z = 1, x < p, 1-x = q$, and no solution to the self-consistent equation for x (17). Thus, this phase is also bounded by the line $q = (1 - p)$, a line (different from the one above) coming from the limits of the numerical solution of (17) and a line already identified as a boundary for the R phase (22). The second line corresponds to the part of the M boundary not already matched by the LM boundary

$$L_r q g(1) = L_\ell (1 - q) g((1 - q)/p). \tag{24}$$

Note that if the lengths of the left and right branches are the same, as chosen for the system from which data are presented in figure 3(*a*), this phase is symmetric with the LM phase.

LR phase. Finally, for condensates situated on the left and right branches to coexist, the appropriate conditions are $z < 1, x = p, 1 - x = q$, and no solution to the self-consistent equation for x (17). Thus, this phase is bounded by the line $q = 1 - p$, a line from solving (17) which happens to touch, but not cross, $q = 1 - p$ for the case studied here and lines that have already been identified as boundaries for the L and R phases (19) and (21).

As before, the other possible phases (LRM and N) are not observed when the density is sufficiently high, as has been assumed. The LRM phase can again only possibly exist on the line $q = 1 - p$ and it is likely that the condensate will only form on at most two of the sections. Finally, the N phase will not be seen when the density is sufficiently high as the system must take on a condensate to accommodate the number of particles in a steady state.

The phase diagram for a system with $N_{\rm tot} = 8000$, $L = 2000$ and $L_\ell = L_r = 500$ is shown in figure 3(*a*). Also shown are the p and q values for simulations that have been run to verify the phase behaviour.

As before the changes in the phase diagram due to changing the lengths of the branches (which do not have to be the same) are straightforward to compute. The boundary of the LR phase remains unchanged as the line $q = 1 - p$, but the point where the other boundary lines meet with this one does move along this line and the boundaries between the LM and L and LR and L change length and slope accordingly. The boundary lines between the M and the LM and RM phases, respectively, retain their curved shape, but they move and the points at which they touch $q = 1 - p$ and $q = 1$ or $p = 1$ also change.

As in the previous case, the analysis can also be applied to systems with densities that do not *a priori* guarantee the presence of a condensate. Again, however, the application is less straightforward and relies on simultaneous numerical solutions of the density equation (11) and the self-consistent equation for x (17). The phase diagram calculated in this way for the system with $L_\ell = L_r = 500$, $L_m = 1000$ and $N_{\rm tot} = 800$ (i.e., the same system as above but at a lower density) is shown in figure 3(*b*). Here the N phase is realized, the LM and RM phases are lost and the phase diagram has become richer in structure.

Again, how and when the phases emerge as the total number of particles is increased is perhaps more straightforward to calculate than the full phase diagram. Clearly, at low enough particle numbers there will be no condensation in the system. For sufficiently small q (p), the R (L) phase will emerge simply when there are sufficient particles to support such a phase i.e., $N_{\rm tot} = L_r g(1)$ ($L_\ell g(1)$). Likewise, the LR phase will emerge for sufficiently small p and q when $N_{\rm tot} = (L_l + L_r)g(1)$. The M phase must first emerge at $p = q = 1$ when the number of particles on the main stretch first becomes critical, and will do so at $N_{\rm tot} = L_m g(1) + L_r g(1 - x) + L_\ell g(x)$, with x being the solution of $x(L_r g(1 - x) + L_\ell g(x)) = L_r g(1 - x)$. For the symmetric system with $L_m = 1000$, $L_\ell = L_r = 500$ this turns out to be $N_{\rm tot} = 634$. The RM phase emerges from the $p = 1$ boundary when both the right branch and main stretch occupancies first attain their critical values together. This is at the point $N_{\rm tot} = L_r g(1)/(1 - q) + L_m g(1)$, with q coming from the solution of $(1 - q)(L_\ell g(1 - q) + L_r g(1)) = L_r g(1)$; for the specific system from which data are presented in figure 3(*b*) this is $N_{\rm tot} = 860$. Also, for the specific system studied here the RM phase is symmetric with the LM phase. At $N_{\rm tot} = 1000$, the N phase disappears completely as this is the point where the LR, LM and RM phases first meet up i.e., when $N_{\rm tot} = L_\ell g(1) + L_r g(1) + L_m g(1)$. The L and R phases are present for all high particle densities, although they will eventually become infinitesimally small, the thickest part of the phases behaving as $p, q \sim 1/N_{\rm tot}$, respectively.

Finally, we note that although the grand-canonical formalism does not deal directly with the condensates, when x, z become such that one or more condensates are present, they can be inserted as free variables that are capable of taking any value greater than zero in order to satisfy the x-balance and density equations. The solution found in this way will break down only when the x, z solution becomes such that the condition for another phase will be met or when at least one of the condensates has to go to zero to satisfy the equations. Due to the way that the sub-critical occupations of each section depend on z, it can be shown that approaching a boundary from either side must result in an unambiguous answer. Thus, it is expected that many different forms of the x-function will give the kind of multiple condensate behaviour seen for the two choices, (2) and (3), considered in this study. The only constraints which should be placed on a suitable x-function are the following: it has a range between 0 and 1; it gives a unique solution to the self-consistent equation for x and the density equation for any given (p, q) pair; it is repulsive in some way so as to inhibit a sole condensate; and it is sufficiently smooth that the solution will not be discontinuous within any phase.

4. Numerical results

To verify the predicted phase diagrams, we performed extensive Monte Carlo simulations on this system with both feedback mechanisms. Our simulation method is simple: a site is picked at random and a particle there is moved to the next site with the relevant probabilities, (1), (2) and (3). We have studied a range of branch lengths, $N_{\rm tot}$'s, p's, q's and Q's. In this paper, we only present the results of $L_m = 1000$, $0 < p < 1$, $0 < q < 1$, $N_{\rm tot} = \{800, 8000\}$, with $L_\ell = 300$, $L_r = 600$, $Q = 20$ for the system with feedback from the left branch only and $L_\ell = L_r = 500$ for the system with feedback from both branches. In the phase diagrams, shown in figures 2 and 3, we display the behaviour of the condensates. N indicates no condensates are present. If a single condensate appears in the system, its location is denoted by L, R and M—indicating the left, right and main sections, respectively. Similarly, the labelling of coexistence of two condensates is self-explanatory. The lines are predictions of the phase boundaries from our mean-field theory. The crosses (+) indicate points at which simulations have been performed. All numerical results showed the expected behaviour for the relevant phase. Occasionally, small discrepancies between prediction and simulation were seen very close to the boundaries, but in all cases these discrepancies lessened when larger system sizes were used. Note that, since systems with the second feedback mechanism ((3) and figure 3) and with $L_\ell = L_r$ are symmetric under $p \leftrightarrow q$, only one half of the phase diagram (above or below the line $q = p$) was tested.

One phenomenon appeared in the majority of the runs, namely, a tendency for condensates to form on the first site of the section. The reason for this behaviour is neither transparent nor intuitive. The exact solution for the fixed-x system implies that the condensate is equally likely to be found anywhere in the *stationary* state. Clearly, the *dynamics* breaks overall translational invariance, so that the favouring of the first site may be a subtle manifestation of the underlying dynamics. One possible explanation is that fluctuations are expected to travel faster in a sub-critical segment than in a critical one [6, 33]. Thus, if the main stretch is sub-critical and the left-branch is critical, for example, density fluctuations would be transported through the main stretch to the beginning of the left branch faster than they will be transported away from the beginning of the left branch. Exploring this issue is beyond the scope of this work, but would be interesting for future studies. To ensure that other sites are equally favoured, in the steady state, for condensation, we carried out runs where one or more condensates were initially placed at 'interior' sites. It is reassuring that such condensates did not move to the first site. We should emphasize, of course, that the probability for a condensate to appear on any site (of the allowed sections) is equal, so that the condensate will move between sites. Given sufficient time, all sites will eventually be explored in a *finite* system. This wandering behaviour has been observed, especially when a small condensate on one section coexists with a large condensate in another. The large condensate remains stationary, but the smaller one moves between several sites over the duration of the run. This is also consistent with the propagation of fluctuations picture: when the main stretch and left branch are critical, fluctuations are expected to travel at the same speed in both and so will not aggregate at the first site. The mobility of condensates in ZRPs on one-dimensional rings and fully connected geometries has been discussed in [34].

We also considered a more sensitive test for our mean-field theory. Since the predictions from this approach are based on the solution of a system with *fixed* x, we performed simulations on such systems—with x *fixed* at the value expected by theory. In particular, we studied distributions for the occupation of a site on each of the three sections (M,L,R) for both these fixed-x systems and the original model. Comparisons are shown in figures 4 and 5. To be consistent with the theory, these distributions should match everywhere *except* in those parts

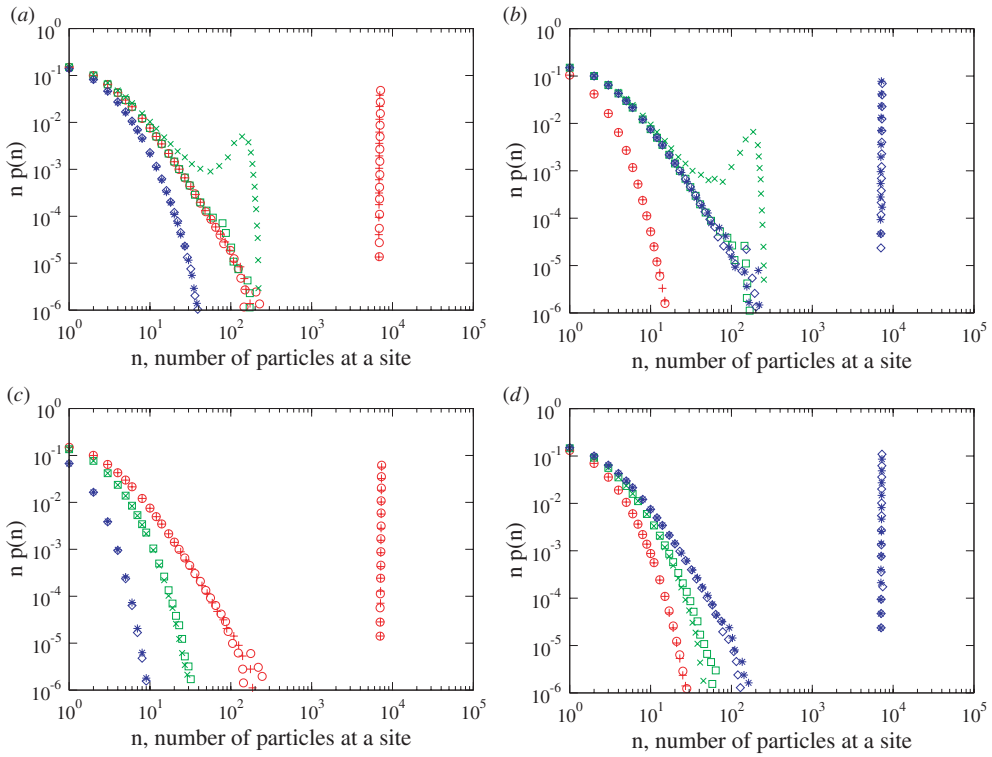

Figure 4. Residence plots of the number of particles on a site in the main stretch, left branch and right branch for the system with branch choice probability, x, dependent on the state of the left branch only (given by the form (2)) compared with the same distributions from a system with the branch choice probability fixed at the value predicted by theory. The system had $L = 1900$ sites with $L_\ell = 300$ and $L_r = 600$, $N_{\rm tot} = 8000$ particles and repulsion parameter $Q = 20$. The distributions are shown for p and q values which fit in the various phases: (*a*) LM phase ($p = 0.25, q = 0.85$), (*b*) LR phase ($p = 0.1, q = 0.5$), (*c*) M phase ($p = 0.9, q = 0.65$), (*d*) R phase ($p = 0.58, q = 0.25$). In all cases the distributions are given for the fixed-x system in the main stretch (○, red online), the left branch (□, green online) and the right branch (◇, blue online) and for the varying-x system in the main stretch (+, red online), the left branch (×, green online) and the right branch (∗, blue online). From the theory, it is expected that the distributions from the system with x fixed and the system with x varying should match, with the exception of the condensate region. This is seen in (*a*) and (*b*) where in the fixed-x system the condensates are on the main stretch and right branch, respectively, and in the varying-x system small amounts of these are shared with a condensate on the left branch. In general, the agreement is very good.

which represent a condensate. Specifically, for the varying-x system at high enough densities, the single condensate characteristic of the fixed-x system can be split into two residing on two different sections of the lattice. In general, the agreement was observed to be excellent. There was some apparent discrepancy when a 'small' condensate was present, but such differences are consistent with finite-size effects observed in the standard ZRP at densities above, but close to, criticality.

We also studied how the quality of the agreement between the theory and simulations depends on the lengths of the branches, focusing only on the second feedback mechanism—x given by (3). We chose $L_\ell = L_r$ in the range of 10–500 sites and ran the system in the LM, LR and M phases. The global density of particles was fixed. We measured both the fractional

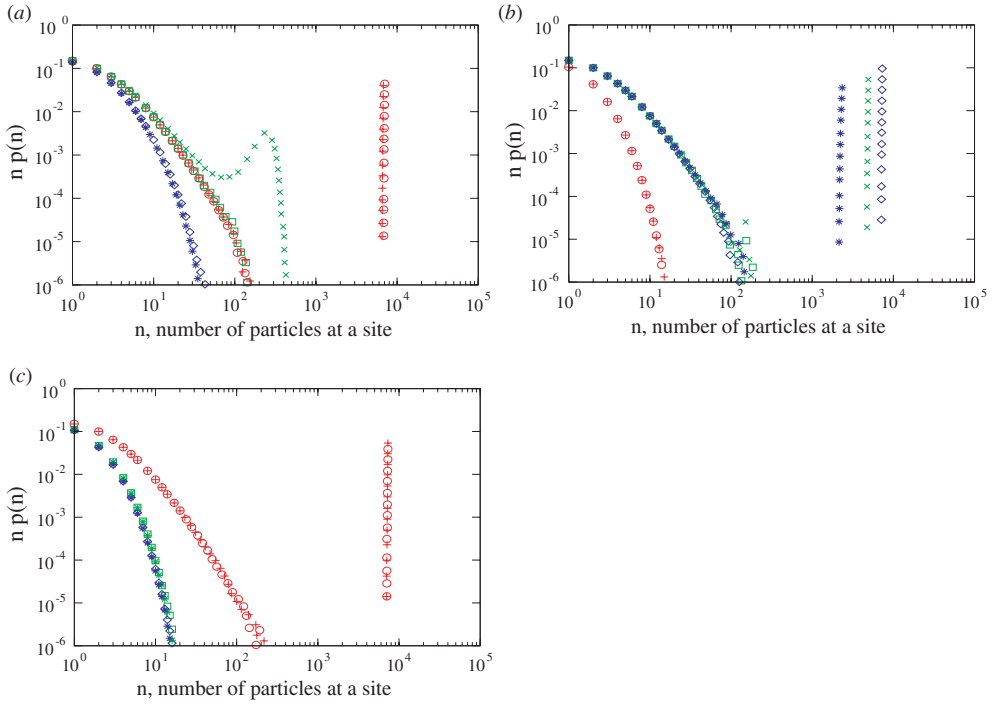

Figure 5. Residence plots of the number of particles on a site in the main stretch, left branch and right branch for the system with branch choice probability, x, dependent on the state of both branches (given by the form (3)) compared with the same distributions for a system with x fixed at the value predicted by theory. The system had $L = 2000$ sites with $L_\ell = L_r = 500$ and $N_{\rm tot} = 8000$ particles. The distributions are shown for p and q values which fit in the phases: (a) LM phase ($p = 0.25, q = 0.85$), (b) LR phase ($p = 0.2, q = 0.4$), (c) M phase ($p = 0.75, q = 0.85$). The RM phase is not represented as this is symmetric with the LM phase. In all cases the distributions are given for the fixed-x system in the main stretch (○, red online), the left branch (□, green online) and the right branch (◇, blue online) and the varying-x system in the main stretch (+, red online), the left branch (×, green online) and the right branch (∗, blue online). From the theory it is expected that the distributions from the system with fixed x and the system with varying x should agree, except for the part of the distribution which describes the condensate. For this system the agreement is very good.

deviation of x from its expected value and the fluctuations in x on the scale of the mean, see figure 6. Generally, the agreement worsens as the branches are shortened. However, this general trend is *not* observed for the LR phase. One possible difference is the following. For the LM and M phases, at least one of the branches will have a low density of occupation, leading to effects of discreteness. In very short branches and with low densities, there are typically only a few particles on the sites, so that changes in occupation happen through comparatively large jumps. Also, the fact that the LM phase deviates and fluctuates more than the M phase is probably due to the fact that the condensate on the left branch is relatively small and so, more susceptible to instability and collapse. For very small branch lengths, some blurring of the phase boundaries was observed. Close to the boundaries expected from theory, the states observed sometimes did not match with those predicted. It is thought that these states may be metastable, as systems artificially nucleated in the expected state remained there for the duration of all runs.

Finally, we also studied numerically the validity of the theory at low densities where no condensation occurs. Through simulations, we can deduce the values of x and z. These values

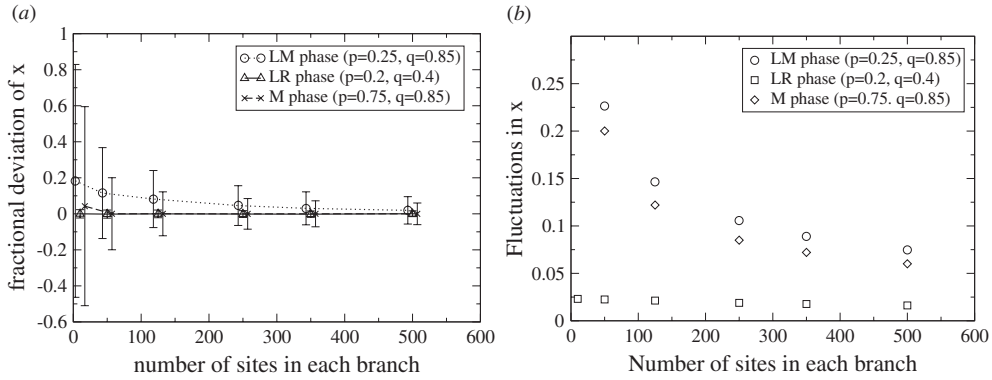

Figure 6. Behaviour of the system with branch choice probability, x, dependent on left and right branches (with the form given by (3) with varying, but equal, numbers of sites in the branches. The system has $L_m = 1000$ sites in the main stretch and a fixed global density of four particles per site. (*a*) The fractional deviation of the branch choice probability, x, from the value predicted by the mean-field theory. (*b*) Standard deviation of the branch choice probability, x, on the scale of the mean.

are then inserted into (14) and (11) to see how well the latter are satisfied. In all cases the agreement is very good. Apparently, the grand-canonical analysis is quite successful for a self-consistent, mean-field approach.

5. Conclusion

In this paper, a generalization of a ZRP with limited long-range interactions was studied. The basic model was that of a ring lattice with a section which splits into two branches at a *T*-junction before rejoining. Apart from the branch point (BP), we impose the standard ZRP rules for totally asymmetric particle hopping. The rates are uniform within each branch, but may be different for the three sections. For the particle at the BP, we must assign probabilities of hopping to each branch. If these are fixed parameters, there exists an exact solution for the stationary state distribution. Here, we focus on a simple generalization, i.e., that these probabilities depend on the total occupation within the branches. Thus, there is a *long-range interaction* between the particle at the BP and those in the branches. We study this system both analytically and with extensive Monte Carlo simulations. Our self-consistent mean-field theory is based on the exact solution with fixed probabilities.

The long-range feedback mechanism has interesting consequences for the system. For systems with sufficiently high densities and fixed branching probabilities, a condensate forms only on one of the three sections. In other words, there can be only four regions in a phase diagram (involving the overall density, the relative hopping rates, and the branching probabilities). By contrast, our model displays three *additional* phases, associated with *coexistence* of condensates on two of the three branches. As a side remark, we note that coexistence of condensates on all three branches can only happen on a line rather than in an extended region in parameter space and is therefore difficult to observe in simulations. As a result, the global phase diagram is considerably richer. Here we have focussed on homogeneous rates in each section, but disordered rates can also produce condensation and the multiple condensate behaviour has also been observed in these systems when feedback is present.

In simulations, we often observe the condensate forming on the first site of a section. This behaviour parallels the one displayed in a ZRP with *open boundaries* [14], in which particles are inserted into the left boundary and extracted from the right boundary with constant rates. If the insertion rate is low and the extraction rate is high, no condensate appears and much can be understood through a treatment similar to the one used here: exploiting a grand-canonical function with fugacities dependent on the boundary rates. For high insertion and/or low extraction rates, condensation was seen on the end sites, but these condensates tended to continue growing with time. In our branching ZRP (with periodic boundary conditions), the formation of a condensate will feedback into the equivalent of the insertion rate and so, a condensate with a stable size can form. The success of the grand-canonical treatment in the open boundary model may be related to the good agreement between the mean-field theory and simulation results in our model.

Remarkably, this agreement continues to be quite good for very short ($\sim$10 sites) branches. This is somewhat surprising, since mean-field theories are expected to be reliable only in the thermodynamic limit. We suspect, however, that the effects due to the finite size of the *main stretch* may be more serious, and we intend to explore these effects in a future publication. In any case, the good agreement we found provides hope that the mean-field approach may be suitable for further generalizations, such as more branches/loops and increasingly complex long-range feedbacks. We believe that, with the promise of further surprises, such systems deserve further investigations. In particular, we believe that there is considerable potential for applying such models to a broad spectrum of physical systems. In particular, there are many transport processes on networks where individual 'agents' make decisions on which route to take, based on the existing state of the rest of the network. Examples include vehicular traffic systems and data transport in computer networks. The model studied here is perhaps the simplest of this class and we hope that it serves as a springboard for complex generalized models and advances the understanding of realistic systems.

Acknowledgments

This work was supported in part by grants from the US National Science Foundation DMR-0414122 and 0705152. We are grateful to the referees for many constructive comments.

References

[1] Spitzer F 1970 *Adv. Math.* **5** 246
[2] Evans M R and Hanney T 2005 *J. Phys. A: Math. Gen.* **38** R195
[3] Evans M R 2000 *Braz. J. Phys.* **30** 42
[4] O'Loan O J, Evans M R and Cates M E 1998 *Phys. Rev.* E **58** 1404
[5] Godrèche C 2003 *J. Phys. A: Math. Gen.* **36** 6313
[6] Großkinsky S, Schütz G M and Spohn H 2003 *J. Stat. Phys.* **113** 389
[7] van Leeuwen J M J and Kooiman A 1992 *Physica* A **184** 79
[8] Carlson J M, Granna E R and Swindle G H 1993 *Phys. Rev.* E **47** 93
[9] Kaupužs J, Mahnke R and Harris R J 2005 *Phys. Rev.* E **72** 056125
[10] Török J 2005 *Physica* A **355** 374
[11] Chowdhury D, Santen L and Schadschneider A 2000 *Phys. Rep.* **329** 199
[12] Helbing D 2001 *Rev. Mod. Phys.* **73** 1067
[13] Kafri Y, Levine E, Mukamel D, Schütz G M and Török J 2002 *Phys. Rev. Lett.* **89** 035702
[14] Levine E, Mukamel D and Schütz G M 2005 *J. Stat. Phys.* **120** 759
[15] Evans M R and Hanney T 2003 *J. Phys. A: Math. Gen.* **36** L441
[16] Hanney T and Evans M R 2004 *Phys. Rev.* E **69** 016107
[17] Schütz G M 2003 *J. Phys. A: Math. Gen.* **36** R339

[18] Großkinsky S and Spohn H 2003 *Bull. Braz. Math. Soc.* **34** 489
[19] Angel A G, Hanney T and Evans M R 2006 *Phys. Rev.* E **73** 016105
[20] Zia R K P, Evans M R and Majumdar Satya N 2004 *J. Stat. Mech.* L10001
[21] Evans M R, Majumdar Satya N and Zia R K P 2004 *J. Phys. A: Math. Gen.* **37** L275
[22] Majumdar Satya N, Evans M R and Zia R K P 2005 *Phys. Rev. Lett.* **94** 180601
[23] Evans M R, Majumdar Satya N and Zia R K P 2006 *J. Stat. Phys.* **123** 357
[24] Evans M R, Majumdar Satya N and Zia R K P 2006 *J. Phys. A: Math. Gen.* **39** 4859
[25] Noh J D, Shim G M and Lee H 2005 *Phys. Rev. Lett.* **94** 198701
[26] Noh J D 2006 *Phys. Rev.* E **72** 056123
[27] Tang M, Liu Z H and Zhou J 2006 *Phys. Rev.* E **74** 036101
[28] Waclaw B, Bogacz L, Burda Z and Janke W 2007 *Preprint* cond-mat/0703243
[29] Bogacz L, Burda Z, Janke W and Waclaw B 2007 *Preprint* cond-mat/0701553
[30] Quince C, Higgs P G and McKane A J 2005 *Ecol. Modelling* **187** 389
[31] Andjel E D 1982 *Ann. Probab.* **10** 525
[32] Andrews G E, Askey R and Roy P 1999 *Special Functions (Encyclopedia of Mathematics and its Applications* vol 71*)* ed G-C Rota (Cambridge: Cambridge University Press)
[33] Schütz G M and Harris R J 2007 *J. Stat. Phys.* **127** 419
[34] Godrèche C and Luck J M 2005 *J. Phys. A: Math. Gen.* **38** 7215